J. Am. Chem. Soc. 1984, 106, 1986-1991

Metal–Nitroxyl Interactions. 38. Effect of the Nickel–Nitroxyl Linkage on the Electron–Electron Spin–Spin Interaction in Fluid and Frozen Solution

Paul H. Smith, Gareth R. Eaton,* and Sandra S. Eaton

Contribution from the Departments of Chemistry, University of Denver, Denver, Colorado 80208, and University of Colorado at Denver, Denver, Colorado 80202. *Received September 19, 1983*

Abstract: A series of spin-labeled nickel(II) complexes has been prepared with zero, one, two, four, and six CH_2 groups between a piperidinyl nitroxyl ring and a nickel xanthate ring. The electron–electron spin–spin interaction decreased rapidly as the number of CH_2 groups was increased. The line widths of the nitroxyl signals in the EPR spectra of the complexes with zero or one CH_2 group increased as the temperature was decreased, which is consistent with incomplete motional averaging of an anisotropic spectrum. For the complexes with two, four, or six CH_2 groups the nitroxyl line widths in 2:1 toluene:chloroform solution were substantially sharper at low temperature (−60 °C) than at room temperature. A similar decrease in the line widths was observed in a solvent mixture with a microviscosity at room temperature similar to that of 2:1 toluene:chloroform at −60 °C. Therefore the decrease in the line widths at low temperature was attributed to a decrease in the segmental mobility of the molecules. The large shifts in the nitroxyl lines in the frozen solution EPR spectra of the compounds with zero or one CH_2 group indicate that exchange makes a significant contribution to the spin–spin interaction.

When the slowly relaxing $S = {}^1/_2$ transition-metal ions Cu(II), Ag(II), VO(IV), and low-spin Co(II) interact with a nitroxyl spin label, high-resolution electron spin-electron spin splitting (AB patterns) is observed in the EPR spectra.[1-5] Far less is known about the impact on a nitroxyl EPR spectrum of an intramolecular interaction with a rapidly relaxing transition metal. A number of nonquantitative reports in the Russian literature have indicated that EPR spectra were not observed for spin-labeled complexes of paramagnetic nickel(II) in fluid solution and/or in polycrystalline samples.[6-18] In all of those cases the structure of the nitroxyl ligand was such that a strong nickel–nitroxyl interaction would be expected.

We recently reported that in the fluid-solution EPR spectra of the six-coordinate pyridine and 2,2′-bipyridine adducts of I and II, the nickel–nitroxyl interaction caused a disappearance of the normal three-line nitroxyl spectrum.[19] In these molecules the through-bond pathway between the nickel and the nitroxyl is relatively direct, and strong spin–spin interaction would be expected. It was of interest to determine how an extension of the nickel–nitroxyl chain would effect the nickel–nitroxyl interaction. We have therefore prepared III–V. In this paper we report the EPR spectra of the six-coordinate adducts of I–V in fluid solution as a function of temperature and in frozen solution.

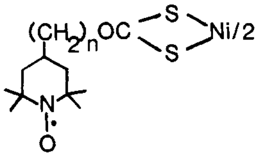

n	
0	I
1	II
2	III
4	IV
6	V

Experimental Section

Physical Measurements. Visible spectra were obtained on a Beckman Acta V spectrophotometer. Infrared spectra were obtained on a Perkin-Elmer 283B infrared spectrophotometer. Melting points were obtained in air on a Thomas Hoover capillary melting point apparatus and are uncorrected. Elemental analyses were performed by Spang Microanalytical Laboratory. Eastman 13181 Silica Gel plates with diethyl ether as eluant were used for all TLC unless otherwise noted. EPR spectra were obtained on a Varian E-9 spectrometer with an E-231 cavity and a variable-temperature Dewar insert in the cavity. The spectrometer is interfaced to a Varian 620/L-103 minicomputer. Spectra were obtained in 4-mm quartz tubes on air-saturated solutions. The ethanol stabilizer in chloroform was removed by passing it through Baker 0537 alumina immediately prior to preparing solutions. The nickel concentrations in the solutions were about 2.0×10^{-3} M. Spectra of the pyridine and 2,2′-bipyridine adducts were obtained on solutions containing about 0.32 M pyridine or 2.3×10^{-3} M 2,2′-bipyridine (bipy), respectively.

Preparation of Compounds. Compounds I and II were prepared as previously reported.[19]

2-(2,2,6,6-Tetramethyl-1-oxy-4-piperidinylidene)acetic Acid Ethyl Ester (VI). This compound was prepared by a procedure similar to that reported by Kosman and Piette.[20] 1,2-Dimethoxyethane (DME) (30

---

* Address correspondence to this author at the University of Denver.

(1) Eaton, S. S.; Eaton, G. R. *Coord. Chem. Rev.* **1978**, *26*, 207–262.

(2) More, K. M.; Eaton, S. S.; Eaton, G. R. *J. Am. Chem. Soc.* **1981**, *103*, 1087–1090.

(3) Sawant, B. M.; Shroyer, A. L. W.; Eaton, G. R.; Eaton, S. S. *Inorg. Chem.* **1982**, *21*, 1093–1101.

(4) More, J. K.; More, K. M.; Eaton, G. R.; Eaton, S. S. *Inorg. Chem.* **1982**, *21*, 2455–2460.

(5) Eaton, S. S.; Boymel, P. M.; Sawant, B. M.; More, J. K.; Eaton, G. R. *J. Magn. Reson.*, in press.

(6) Sagdeev, R. Z.; Molin, Yu. N.; Kutikova, G. A.; Volodarsky, L. B. "Proceedings, XVIth Colloque Ampere, Bucharest"; 1970, p 1159–1161.

(7) Sagdeev, R. Z.; Molin, Yu. N.; Salikov, R. A.; Volodarsky, L. B.; Kutikova, G. A. *J. Magn. Reson.* **1973**, *9*, 13–26.

(8) Jahr, D.; Rebhan, R. H.; Schwarzhans, K. E.; Wiedemann, J. *Z. Naturforsch., B: Anorg. Chem., Org. Chem.* **1973**, *B28*, 55–62.

(9) Larionov, S. V.; Ovcharenko, V. I.; Sadykov, R. A.; Sagdeev, R. Z.; Volodarskii, L. B. *Koord. Khim.* **1975**, *1*, 1312–1316; *Sov. J. Coord. Chem.* (*Engl. Transl.*) **1975**, *1*, 1094–1097.

(10) Larionov, S. V.; Ovcharenko, V. I.; Kirichenko, V. N.; Sagdeev, R. Z.; Volodarskii, L. B. *Koord. Khim.* **1978**, *4*, 1878–1883; *Sov. J. Coord. Chem.* (*Engl. Transl.*) **1978**, *4*, 1445–1449.

(11) Ovcharenko, V. I.; Larionov, S. V.; Sadykov, R. A.; Sagdeev, R. Z.; Grigor'ev, I. A.; Volodarskii, L. B. *Koord. Khim.* **1977**, *3*, 1558–1563; *Sov. J. Coord. Chem.* (*Engl. Transl.*) **1977**, *3*, 1218–1222.

(12) Sadykov, R. A.; Sagdeev, R. Z.; Molin, Yu. N.; Ovcharenko, V. I.; Larionov, S. V.; Volodarskii, L. B. *Koord. Khim.* **1977**, *3*, 71–76; *Sov. J. Coord. Chem.* (*Engl. Transl.*) **1977**, *3*, 54–58.

(13) Solozhenkin, P. M.; Shvengler, F. A.; Rakitina, E. V. *Dokl. Akad. Nauk Tadzh. SSR* **1977**, *20*, 25–27.

(14) Ovcharenko, V. I.; Larionov, S. V.; Sagdeev, R. Z.; Volodarskii, L. B. *Izv. Sib. Otd. Akad. Nauk SSSR, Ser. Khim. Nauk* **1978**, 79–84.

(15) Larionov, S. V.; Ovcharenko, V. I.; Sagdeev, R. Z. *Koord. Khim.* **1979**, *5*, 1034–1037; *Sov. J. Coord. Chem.* (*Engl. Transl.*) **1979**, *5*, 814–817.

(16) Larionov, S. V.; Mironova, G. N.; Ovcharenko, V. I.; Volodarskii, L. B. *Izv. Akad. Nauk. SSSR, Ser. Khim.* **1980**, 977–982; *Bull. Acad. Sci. USSR, Div. Chem. Sci.* (*Engl. Transl.*) **1980**, 686–690.

(17) Rzaev, A. A.; Medzhidov, A. A.; Mamedov, Kh. S. *Zh. Neorg. Khim.* **1980**, *25*, 1277–1281; *Russ. J. Inorg. Chem.* (*Engl. Transl.*) **1980**, *25*, 711–713.

(18) Ovcharenko, V. I.; Larionov, S. V. *Zh. Neorg. Khim.* **1981**, *26*, 2758–2762; *Russ. J. Inorg. Chem.* (*Engl. Transl.*) **1981**, *26*, 1477–1479.

(19) Hafid, S.; Eaton, G. R.; Eaton, S. S. *J. Magn. Reson.* **1983**, *51*, 470–476.

0002-7863/84/1506-1986$01.50/0

mL), freshly distilled from lithium aluminum hydride (LAH), was added to 0.39 g (9.0 mmol) of a 56% mineral oil dispersion of sodium hydride under nitrogen, resulting in a cloudy gray mixture. After the mixture was cooled in an ice bath, 1.8 mL (9.0 mmol) of triethyl phosphonoacetate in approximately 5 mL of DME was added over 5–10 min. Evolution of gas was observed. Approximately one hour of stirring at room temperature resulted in a clear colorless solution. The solution was cooled in an ice bath, and 1.53 g (9.0 mmol) of 4-oxo-2,2,6,6-tetramethyl-1-oxy-piperidine (tempone) dissolved in 5 mL of DME was added dropwise over 5 min. After stirring for 20 min at room temperature, 50 mL of ice cold water was added. The resulting mixture was extracted 4 times with 25-mL portions of diethyl ether, and the combined ether layers were extracted 5 times with 20-mL portions of ice cold water. The red-orange ether layer was dried over magnesium sulfate and filtered, and the solvent was removed on a rotary evaporator. The remaining red oil was chromatographed on neutral alumina (Baker 0537) in benzene. The red major band (broad) was collected, and the benzene was removed on a rotary evaporator. The resulting oil was distilled in a one-piece microdistillation apparatus, and the fraction boiling at 98–110 °C at 0.4 mmHg (oil bath temperature of 145–190 °C) was collected in an ice-cooled flask. The product was a red oil (1.08 g, 50%): IR (neat) 1720 (C=O), 1665 (C=C) cm^{-1}.

2-(2,2,6,6-Tetramethyl-1-oxy-4-piperidinyl)acetic Acid Ethyl Ester (VII). VI (1.0 g) was dissolved in 25 mL of 100% ethanol in a Parr shaker bottle, and 28 mg of platinum oxide (Adam's catalyst) was added. The mixture was shaken at 60 psi H_2 for 15 min. Platinum oxide (31 mg) was added to the colorless solution. The vessel was shaken at 60 psi H_2 for approximately 30 h. The reaction was monitored by the disappearance of the C=C IR band at 1665 cm^{-1}. After the solution was filtered through Celite and the ethanol was removed on a rotary evaporator, the resulting yellow oil was taken up in chloroform and lead dioxide (2.0 g) was added. The mixture was refluxed for 3 h and filtered through Celite, and the chloroform was removed on a rotary evaporator leaving a red oil. The oil was chromatographed on silica gel in chloroform. The red band was collected, and the chloroform was evaporated to afford 0.716 g (70%) of red oil: IR (neat) 1740 (C=O) cm^{-1}; TLC R_f 0.62.

2-(2,2,6,6-Tetramethyl-1-oxy-4-piperidinyl)ethanol (VIII). VII (0.716 g, 3.0 mmol) was dissolved in 30–40 mL ether (freshly distilled from LAH) under nitrogen. After cooling the red solution in an ice bath 3.6 mL (1.5 mmol) of 0.42 M LAH solution in ether (prepared and standardized by the method of Vogel)[21] was added dropwise over 4–5 min with an ice-cooled syringe through a rubber septum. A white precipitate formed. The mixture was stirred in the ice bath for 10–15 min. and then 0.23 mL of water was added. After the mixture was warmed to room temperature and the precipitate was broken up with a stirring rod, the mixture was filtered and the ether was removed on a rotary evaporator. The resulting red oil was chromatographed on silica gel (Mallinckrodt 7087) in chloroform, and the eluant was monitored by TLC. The broad red band was collected in two portions, the latter of which contained product. The chloroform was evaporated to afford 0.30 g (50%) of red oil: IR (neat) 3440 (OH) cm^{-1} (br); TLC R_f 0.37.

Potassium 2-(1-(2,2,6,6-Tetramethyl-1-oxy-4-piperidinyl))ethylxanthate (IX). This compound was prepared by the following procedure which is similar to that reported previously for the preparation of potassium (2,2,6,6-tetramethyl-1-oxy-4-piperidinyl)xanthate.[19,22] VIII (0.30 g, 1.5 mmole) was dissolved in approximately 3 mL of carbon disulfide and 0.2 mL of 12.5 M (2.5 mmol) potassium hydroxide solution was added. The mixture (two phases) was stirred at room temperature for 3 h. The precipitate which formed was collected by filtration and washed with diethyl ether. After drying briefly under vacuum the off-white powder was dissolved in 10 mL of acetone, and the volume was reduced to 2–3 mL. Upon addition of diethyl ether a cloudy white precipitate formed, which was collected by filtration, washed with ether, and dried under vacuum: yield 0.19 g (40%); IR (KBr pellet) 1070 (br), 1182, 1245, 1365, 1460, 2930, 2980 cm^{-1}; mp 206–212 °C (dec).

Bis(1-(2,2,6,6-tetramethyl-1-oxy-4-piperidinyl)-2-ethylxanthato)nickel(II) (III). This compound was prepared by the following procedure, which is similar to that reported previously for the preparation of I.[19,22] IX (0.15 g, 0.47 mmol) was dissolved in about 4 mL of water and 1.0 mL of 0.25 M (0.25 mmol) aqueous nickel(II) acetate solution was added. The green precipitate which formed immediately was extracted into chloform, and the combined chloroform layers (about 20 mL total) were dried over sodium sulfate. The dark green solution was filtered, and the chloroform was evaporated leaving a dark oil. The oil was crystallized from a chloroform/heptane mixture by slowly evaporating the chloroform on a rotary evaporator. The reddish brown fluffy solid was collected by filtration, washed with heptane and pentane, and dried under vacuum at room temperature overnight (0.11 g, 77%): IR (KBr pellet) 385, 1140, 1270 (br), 1365, 1407, 2935, 2979 cm^{-1}; vis (chloroform) 479 (log ϵ = 3.26), 418 nm (log ϵ = 3.49); mp 127–129 °C. Anal. Calcd for $C_{24}H_{42}N_2O_4S_4Ni$ with 4.2% C_7H_{16}: C, 48.82; H, 7.33; N, 4.40; S, 20.16. Found: C, 48.82; H, 7.29; N, 4.41; S, 20.15. In another preparation the product was dried extensively under vacuum at 80 °C in order to remove solvent, but the elemental analysis and EPR indicated substantial decomposition.

4-(2,2,6,6-Tetramethyl-1-oxy-4-piperidinylidene)-2-butene-1-carboxylic Acid Ethyl Ester (X). The procedure for the preparation of this compound was similar to that for VI with the following modifications. The Wittig reagent was triethyl 4-phosphonocrotonate. After the addition of tempone, the mixture was stirred for 1 h, before adding the cold water. The fraction boiling at approximately 145 °C at 0.2 mmHg was collected: yield 29% (red oil); IR (neat) 1620 (C=C), 1648 (C=C), 1715 (C=O) cm^{-1}.

4-(2,2,6,6-Tetramethyl-1-oxy-4-piperidinyl)butanoic Acid Ethyl Ester (XI). The procedure for the preparation of XI from X was similar to the procedure used to prepare VII from VI. The modifications were as follows. The initial phase of the hydrogenation was at 45 psi for 30 min. The second phase was at 45 psi for 17 h. The reaction was monitored by the disappearance of the UV band at 270 nm (log ϵ = 4.36). The product was chromatographed on silica gel in chloroform and then on alumina in benzene: yield 17%; IR (neat) 1740 (C=O) cm^{-1}; TLC R_f 0.62.

4-(2,2,6,6-Tetramethyl-1-oxy-4-piperidinyl)butanol (XII). This compound was prepared from XI by a procedure analogous to that used to prepare VIII from VII. In the chromatographic purification, the second red band was collected: yield 66%; IR (neat) 3430 (OH) cm^{-1} (br); TLC R_f 0.41.

Potassium 4-(1-(2,2,6,6-Tetramethyl-1-oxy-4-piperidinyl))butyl Xanthate (XIII). This compound was prepared from XII by a procedure analogous to that used to prepare IX from VIII: yield 37%; IR (nujol mull) 1090 cm^{-1} (br); mp 166–170 °C (dec).

Bis(1-(2,2,6,6-tetramethyl-1-oxy-4-piperidinyl)-4-butylxanthato)nickel(II) (IV). This compound was prepared from XIII by a procedure analogous to that used to prepare III from IX. The product was a dark green-brown crystalline solid which was dried under vacuum at 80 °C for 3 days: yield 69%; IR (KBr pellet) 389, 1043, 1268, 1395, 1469, 2930 cm^{-1}; vis (chloroform) 478 (log ϵ = 3.27), 418 nm (log ϵ = 3.50); mp 113–117 °C. Anal. Calcd for $C_{28}H_{50}N_2O_4S_4Ni$: C, 50.52; H, 7.57; N, 4.21; S, 19.27. Found: C, 50.50; H, 7.66; N, 4.29; S, 19.26.

2-(2,2,6,6-Tetramethyl-1-oxy-4-piperidinyl)acetaldehyde (XIV). The procedure used to prepare this compound is analogous to that reported by Hideg et al. for the preparation of formyl derivatives of pyrroline and pyrrolidine nitroxyls.[23] Pyridinium dichromate (4.28 g, 12.3 mmol) was added to 1.23 g (6.1 mmol) of VIII dissolved in 10 mL of dichloromethane (freshly distilled from phosphorus pentoxide), and the mixture was stirred for 6 h at room temperature. The R_f of the product was larger than that of the starting material. When the TLC indicated that the reaction was complete, the mixture was diluted with about 15 mL of diethyl ether and the dark precipitate was discarded. The solvent was removed on a rotary evaporator, and the reddish oil was chromatographed on silica gel in chloroform. The first red band was collected and the chloroform was evaporated. The resulting red oil was dried under vacuum overnight (0.73 g, 60%): IR (neat) 1728, 2730 cm^{-1}; TLC R_f 0.60.

6-(2,2,6,6-Tetramethyl-1-oxy-4-piperidinyl)-2,4-hexanediene-1-carboxylic Acid Ethyl Ester (XV). This compound was prepared from XIV and triethyl 4-phosphonocrotonate by a procedure analogous to that used to prepare VI from tempone. The red oil obtained after chromatography on alumina in benzene was used in the following reaction without further purification: yield 64%; IR (neat) 1620 (C=C), 1645 (C=C), 1723 (C=O) cm^{-1}.

6-(2,2,6,6-Tetramethyl-1-oxy-4-piperidinyl)hexanoic Acid Ethyl Ester (XVI). This compound was prepared from XV by a procedure analogous to that used to prepare VII from VI. The second phase of the hydrogenation was done at 60 psi for about 18 h. The progress of the reaction was monitored by the disappearance of the C=C IR bands at 1620 and 1645 cm^{-1}: yield 77% (red oil); IR (neat) 1742 (C=O) cm^{-1}; TLC R_f 0.65.

6-(2,2,6,6-Tetramethyl-1-oxy-4-piperidinyl)hexanol (XVII). This compound was prepared from XVI by a procedure analogous to that used

---

(20) Kosman, D. J.; Piette, H. *Chem. Commun.* **1969**, 926–927. Kosman, D. J., personal communication, Feb., 1983.

(21) Vogel "Textbook of Practical Organic Chemistry", 4th ed.; Longman Group Limited: London, 1978; p 301. Benzene was replaced by toluene.

(22) Kirichenko, L. N.; Medzhidov, A. A. *Izv. Akad. Nauk SSSR, Ser. Khim.* **1969**, 2849–2851; *Bull. Acad. Sci. USSR, Div. Chem. Sci.* (*Engl. Transl.*) **1969**, 2685–2687.

(23) Hideg, K.; Hankovszky, H. O.; Lex, L.; Kulcsar, Gy. *Synthesis* **1980**, 911–914.

Scheme I

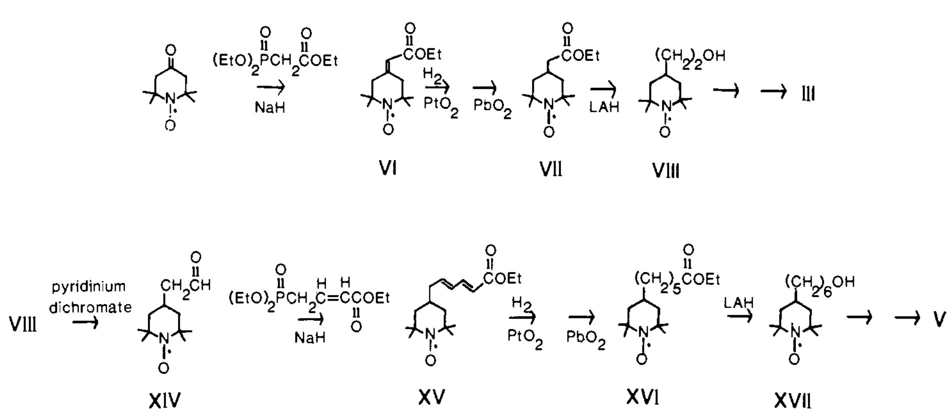

to prepare VIII from VII: yield 64% (red oil); IR (neat) 3440 (OH) cm^{-1} (br); TLC R_f 0.46.

Potassium 6-(1-(2,2,6,6-Tetramethyl-1-oxy-4-piperidinyl))hexyl Xanthate (XVIII). This compound was prepared from XVII by a procedure analogous to that used to prepare IX from VIII: yield 22%; IR (KBr pellet) 1090 (br), 1245, 1362, 1468, 2930 cm^{-1}.

Bis(1-(2,2,6,6-tetramethyl-1-oxy-4-piperidinyl)-6-hexylxanthato)nickel(II) (V). This compound was prepared from XVIII by a procedure analogous to that used to prepare III from IX. The oil was crystallized from a chloroform/heptane mixture by allowing the chloroform to evaporate slowly from a watchglass. The light green crystals were collected by filtration, washed with heptane and pentane, and dried under vacuum at room temperature for approximately 24 h: IR (KBr pellet) 390, 1038, 1261, 1472, 2930 cm^{-1}; vis (chloroform) 479 (log ϵ = 3.23), 417 nm (log ϵ = 3.48); mp 95–99 °C (dec). Anal. Calcd for $C_{32}H_{58}N_2O_4S_4Ni$: C, 53.25; H, 8.10; N, 3.88; S, 17.77. Found: C, 53.19; H, 8.21; N, 3.94; S, 17.75.

Results and Discussion

Synthesis of Compounds. To examine the effect of the length of the linkage between the nickel and the nitroxyl on the magnitude of the electron–electron spin–spin interaction, we have prepared a series of spin-labled nickel xanthate complexes with 0, 1, 2, 4, and 6 CH_2 groups between the nitroxyl ring and the xanthate moiety. The sequences of steps used to prepare the precursors for III and V are shown in Scheme I. Reaction of tempone with a Wittig reagent gave unsaturated acid ester VI. Reduction of the exocyclic double bond and reoxidation of the nitroxyl group gave saturated acid ester VII, which was converted to alcohol VIII with lithium aluminum hydride. Alcohol VIII was converted to spin-labeled nickel xanthate III. A similar series of reactions with a longer chain Wittig reagent gave spin-labeled nickel xanthate IV. Alcohol VIII was oxidized to the corresponding aldehyde XIV. Aldehyde XIV was then used in a series of reactions similar to those outlined for the preparation of VIII, to prepare alcohol XVII and spin-labeled nickel xanthate V. The visible and infrared spectra of I–V were in good agreement with literature data on nickel xanthates.[24,25] The complexes were stable under ordinary conditions but decomposed when heated for prolonged periods in vacuum.

In the square-planar complexes I–V the nickel(II) is diamagnetic. The EPR spectra of I–V were typical three-line nitroxyl spectra, and double integration of the spectra was used as a criterion of the purity of the compounds. Addition of pyridine or 2,2′-bipyridine to solutions of I–V results in formation of 6-coordinate complexes in which the nickel is paramagnetic. The concentrations of pyridine and 2,2′-bipyridine in the solutions were chosen such that greater than 99% of the nickel was in the paramagnetic six-coordinate form.

EPR Spectra in Fluid Solution. X-band EPR spectra of the 2,2′-bipyridine adducts of I–V in 2:1 toluene:chloroform solution at room temperature are shown in Figure 1. In each of the spectra there is a small contribution from a sharp three-line nitroxyl signal due to the equilibrium concentration of the four-coordinate complex in which the nickel is diamagnetic. The nitroxyl lines in the spectrum of I·bipy are severely broadened and extend over about 1000 G. Decreasing broadening is observed as the length of the chain is extended. Similar spectra were observed for the pyridine

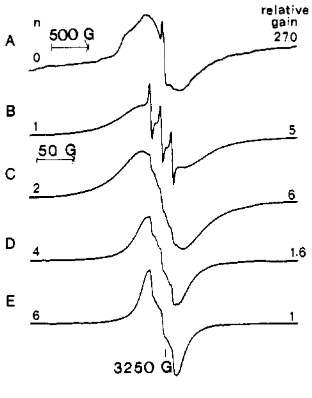

Figure 1. X-band EPR spectra of the bipyridine adducts of I–V in 2:1 chloroform solution at room temperature: (A) 4000-G scan of the spectrum of I·bipy obtained with 40-mW power and 5-G modulation amplitude; (B) 400-G scan of the spectrum of II·bipy obtained with 40-mW power and 2.5-G modulation amplitude; (C) 400-G scan of the spectrum of III·bipy obtained with 8-mW power and 4-G modulation amplitude; (D) 400-G scan of the spectrum of IV·bipy obtained with 20-mW power and 1.25-G modulation amplitude; (E) 400-G scan of the spectrum of V·bipy obtained with 20-mW power and 0.8-G modulation amplitude. As displayed in the figure, the relative amplifications of the five spectra are 270, 5, 6, 1.2, and 1. If the broad signal in B had been scaled to the same amplitude as the other broad signals its relative amplification would be about 10.

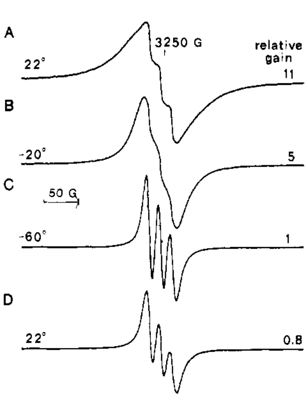

Figure 2. 400-G scans of the EPR spectra of III·(py)$_2$: (A–C) obtained in 2:1 toluene:chloroform solution at 20, −20, and −60 °C, respectively; (D) obtained in 7:3 di-*o*-xylylethane:pyridine solution at room temperature. The microwave powers and modulation amplitudes for the 4 spectra were as follows: A, 20 mW, 1 G; B, 10 mW, 1 G; C, 10 mW, 0.63 G; D, 40 mW, 0.63 G. As displayed in the figure, the relative amplifications of the four spectra are 11, 5, 1, and 0.8.

---

(24) Nanjo, M.; Yamasaki, T. *J. Inorg. Nucl. Chem.* **1970**, *32*, 2411–2422.

(25) Watt, G. W.; McCormick, B. J. *Spectrochim. Acta* **1965**, *24*, 753–761.

Table I. Temperature Dependence of Nitroxyl Line Widths

			L = (pyridine)$_2$		L = bipyridine	
compd	solvent	temp	W[a]	σ[b]	W[a]	σ[b]
II·L	T/C[c]	22			63	22
		−60			70	15
III·L	T/C[c]	22	57	26	52	10
		−60	10	0	11	0
	XE[d]	22	12	0		
IV·L	T/C[c]	22	25	9	26	5
		−60	3	0	4	0
	XE[d]	22	6	0		
V·L	T/C[c]	22	15	0	17	0
		−60	3	0	3	0
	XE[d]	22	4	0		

[a] Peak to peak width of center line of nitroxyl triplet in Gauss. [b] Width of Gaussian distribution of line widths. [c] 2:1 toluene: chloroform. [d] 7:3 di-*o*-xylylethane:pyridine.

adducts. Thus the nickel–nitroxyl interaction results in a broadening of the nitroxyl lines which decreases as the value of *n* increases. When the temperature was decreased, the spectra of I·bipy and II·bipy broadened, which is consistent with incomplete motional averaging of anisotropic spectra. However, for the pyridine or 2,2′-bipyridine adducts of III–V, the spectra narrowed as the temperature was decreased. The spectra of III·(py)$_2$ as a function of temperature which are shown in Figure 2 are typical of the changes that were observed. When the concentration of III·(py)$_2$ was decreased by a factor of 4 the nitroxyl line width at room temperature was unchanged. Therefore intermolecular collisions have a negligible impact on the line widths at these concentrations, and the temperature dependence of the line widths cannot be attributed to a decrease in intermolecular collisions at lower temperatures.

Computer simulation of the room-temperature EPR spectra of the 6-coordinate spin-labeled complexes indicated that most of the spectra were inconsistent with a simple Lorentzian line shape. However, good agreement between observed and calculated line shapes could be obtained by assuming a Gaussian distribution of line widths and Lorentzian line shapes. The distribution was centered at a line width W and the width of the distribution was σ. In simulating the spectra the value of σ was minimized. The nitroxyl nitrogen hyperfine coupling constant was kept between 15.8 and 17.0 G, which are the values observed at room temperature and −60 °C, respectively, in the spectra with resolved hyperfine. The values of W and σ used to simulate the spectra at room temperature and at −60 °C are given in Table I.

To test the possibility that the temperature dependence of the spectra of the compounds with n = 2, 4, and 6 was due to increasing viscosity at low temperature, spectra were obtained in a 7:3 mixture of di-*o*-xylylethane and pyridine. The spectrum of III·(py)$_2$ at −60 °C in 2:1 toluene:chloroform solution (Figure 2C) is similar to that obtained in the viscous solvent mixture at room temperature (Figure 2D). Nitroxyl tumbling rates have been used as a measure of the microviscosity of a solution. The tumbling correlation time (τ) of a nitroxyl can be estimated from the relative widths of the three hyperfine lines.[26,27] The line widths were obtained by computer simulation and fit to the equation $\Delta H(I) = A + Bm_I + Cm_I^2$. The values of B and C were substituted into eq 1 and 2, respectively, to obtain values of τ.[28]

$$\tau_B = (1.3 \times 10^{-9})B \text{ s/rad} \qquad (1)$$

$$\tau_C = (1.2 \times 10^{-9})C \text{ s/rad} \qquad (2)$$

Table II. Nitroxyl Tumbling Correlation Times[a]

			L = (pyridine)$_2$		L = bipyridine	
compd	solvent	temp	τ_B[b]	τ_C[c]	τ_B[b]	τ_C[c]
III·L	T/C[d]	−60	9.8	6.6	9.8	6.6
	XE[e]	22	12	8.4		
IV·L	T/C[d]	−60	12	8.4	12	7.2
	XE[e]	22	13	7.2		
V·L	T/C[d]	−60	9.1	5.6	8.5	6.6
	XE[e]	22	12	6.0		

[a] In units of 10^{-10} s/rad. [b] Value of τ obtained from eq 1. [c] Value of τ obtained from eq 2. [d] 2:1 toluene:chloroform. [e] 7:3 di-*o*-xylylethane:pyridine.

The values obtained for τ in 2:1 toluene:chloroform at −60 °C and in 7:3 di-*o*-xylylethane:pyridine at room temperature are given in Table II. For each of the complexes the values are strikingly similar for the two sets of conditions, which indicates that the microviscosities of the two solutions are about the same. The similarities in the nitroxyl line widths (Table I) and microviscosities for solutions in 2:1 toluene:chloroform at −60 °C and for 7:3 di-*o*-xylylethane:pyridine at room temperature suggest that the dominant effect of temperature on the line widths is due to the change in the viscosity of the solvent. The viscosity could influence the system in seveal ways. For the compounds with n = 0 and n = 1 the increase in viscosity caused an increase in line width which is attributed to incomplete motional averaging of an anisotropic signal. However, the decreasing line widths for the complexes with n = 2, 4, and 6 must arise from a different phenomenon.

In flexible biradicals with weak spin–spin interaction it is commonly observed that the EPR spectra are strongly temperature dependent. At low temperature the spectra are characteristic of noninteracting nitroxyls, but as the temperature is increased, "triplet" lines are observed with a relative intensity that increases with increasing temperature. This has been attributed to segmental mobility of the molecule which permits collisional interaction between the two nitroxyl moieties or between one nitroxyl and a portion of the molecule which has a significant population of the spin density from the second nitroxyl.[29] We propose that a similar phenomenon occurs in the nitrogeneous base adducts of spin-labeled nickel complexes III–V. The nickel–nitroxyl interaction through the long hydrocarbon chains is weak but gives rise to some broadening of the nitroxyl lines as is evident in the spectra at −60 °C. However, at higher temperatures segmental mobility permits occasional close encounters between the nitroxyl moiety and the nickel or regions of the molecule on which significant nickel spin density is delocalized. The broadening of the nitroxyl signal is dependent on the frequency of the collisions and the strength of the interaction during the collision. In the high-viscosity solvent the segmental mobility is greatly decreased and the spectra resemble those obtained at a similar microviscosity obtained by lowering the temperature of the toluene:chloroform mixture.

The values of W and σ in Table I can now be considered in light of this proposal. For each of the complexes at −60 °C the value of σ is zero within experimental error and the value of W is smaller than at room temperature. We therefore propose that both the broadening of the lines and the increasing width of the distribution in the line widths with increasing temperature reflect the effects of increasing segmental mobility on the spin–spin interaction. Motions which are intermediate to rapid on the EPR time scale give rise to averaged spectra. Thus an increasing frequency of strong interaction between the nitroxyl and the nickel by molecular motions with low energy barriers results in an increase in the average line width. If the rate of the motion is slow to intermediate on the EPR time scale, then the interconverting species give rise to the distinct EPR spectra. Thus the distribution in the line widths indicates the presence of conformations which are interconverting slowly on the EPR time scale and have different average line widths.

The values of both W and σ at room temperature decrease rapidly as the number of CH_2 groups in the molecule is increased. As the length of the chain increases, the probability of a nitroxyl

---

[26] Kivelson, D. *J. Chem. Phys.* **1960**, *33*, 1094–1106.

[27] Wilson, R.; Kivelson, D. *J. Chem. Phys.* **1966**, *44*, 154–168.

[28] Schreir, S.; Polnaszek, C. F.; Smith, I. C. P. *Biochim. Biophys. Acta* **1978**, *515*, 375–436.

[29] Rozantsev, E. G. "Free Nitroxyl Radicals"; Plenum Press: New York, 1970; p 142–157.

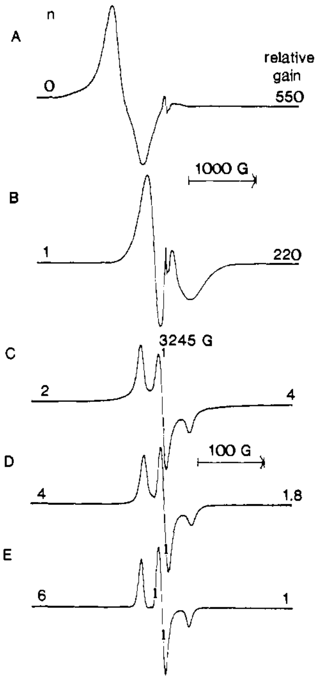

Figure 3. X-band EPR spectra of the pyridine adducts of I–V in frozen 2:1 toluene:chloroform solution (~−180 °C): (A) 4000-G scan of the spectrum of I·$(py)_2$ obtained with 50-mW power and 5-G modulation amplitude; (B) 4000-G scan of the spectrum of II·$(py)_2$ obtained with 50-mW power and 5-G modulation amplitude; (C) 400-G scan of the spectrum of III·$(py)_2$ obtained with 0.1-mW power and 1-G modulation amplitude; (D) 400-G scan of the spectrum of IV·$(py)_2$ obtained with 0.4-mW power and 0.5-G modulation amplitude; (E) 400-G scan of the spectrum of V·$(py)_2$ obtained with 0.01-mW power and 0.8-G modulation amplitude. As displayed in the figure, the relative amplifications of the five spectra are 550, 220, 4, 1.8, and 1.

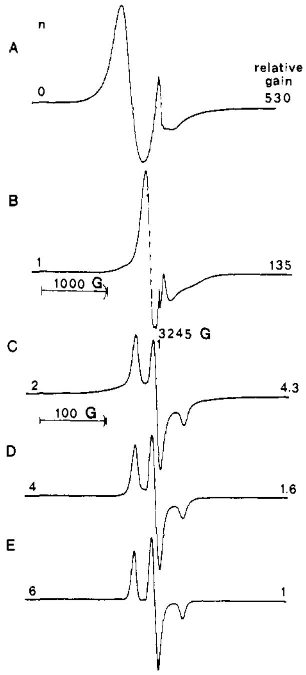

Figure 4. X-band EPR spectra of the bipyridine adducts of I–V in frozen 2:1 toluene:chloroform solution (~−180 °C): (A) 4000-G scan of the spectrum of I·bipy obtained with 50-mW power and 5-G modulation amplitude; (B) 4000-G scan of the spectrum of II·bipy obtained with 50-mW power and 5-G modulation amplitude; (C) 400-G scan of the spectrum of III·bipy obtained with 0.4-mW power and 1-G modulation amplitude; (D), 400-G scan of the spectrum of IV·bipy obtained with 0.1-mW power and 1-G modulation amplitude; (E) 400-G scan of the spectrum of V·bipy obtained with 0.04-mW power and 0.8-G modulation amplitude. As displayed in the figure, the relative amplifications of the five spectra are 530, 135, 4.3, 1.6, and 1.

moiety coming close to a region of the molecule with large nickel spin density is decreased and so the same (or perhaps even greater) motion is not as likely to result in strong spin–spin interaction. The values of W at room temperature for each of the complexes are similar for the pyridine and 2,2′-bipyridine adducts, but the values of σ are substantially larger for the pyridine adducts than for the 2,2′-bipyridine adducts. This suggests that there are a greater variety of slowly interconverting conformations of the pyridine adducts than of the 2,2′-bipyridine adducts. The 2,2′-bipyridine is sterically required to occupy cis positions in the six-coordinate complexes, but the pyridine adducts may be mixtures of cis and trans isomers.

EPR Spectra in Frozen Solution. The EPR spectra of the pyridine adducts of I–V in frozen solution are shown in Figure 3. Similar spectra were obtained for the 2,2′-bipyridine adducts (Figure 4). For both the pyridine and 2,2′-bipyridine adducts of V ($n = 6$) the nitroxyl signal is only slightly different from that observed for a nitroxyl unperturbed by a paramagnetic ion. The amplitudes of the signals are about 80% of that expected in the absence of spin–spin interaction, and the line widths are about 0.5 G greater. The power saturation curve is linear to about 0.2 mW whereas linearity to about 0.1 mW is generally observed for similar concentrations of noninteracting nitroxyls. In mixtures of nitroxyl radicals and bis(ethyl xanthate)nickel dipyridinate at these concentrations, there is negligible intermolecular spin–spin interaction. Thus the weak spin–spin interaction in the adducts of V is intramolecular.

In the six-coordinate adducts of III and IV ($n = 2, 4$) the spectra still exhibit the characteristic three-line nitroxyl pattern but the line shapes are clearly distorted. The double integrals indicated that all of the nitroxyl intensity was present, but the increased line widths necessitated the use of higher gains to obtain signal amplitudes comparable to those expected for noninteracting nitroxyls at the same concentration. The spectra could not be simulated with a single broadened line width. Some features could be reproduced by assuming a distribution of line widths with the line widths along the nitroxyl x and y axes broader than the line width along the z axis. However, that still did not give good agreement with the broad wings on the low-field side of the spectra.

Leigh proposed that dipolar interaction of a nitroxyl with a rapidly relaxing metal would result in a spectrum with a distribution of line widths.[30] A simulation program based on the formulas given in ref 30 gave spectra which agreed fairly well with the reduced amplitude of the spectra and the shape of the center portions of the spectra but did not match the broad low-field wing that is most noticeable in the spectrum in Figure 4C. In Leigh's model the broadening is related to the parameter C which is given by eq 3

$$C = g\beta\mu^2\tau/r^6\hbar \qquad (3)$$

where μ is the magnetic moment of the metal, r is the distance between the metal and the nitroxyl, and τ is the metal T_1. The simulations required the use of C about 4 for IV·bipy and IV·$(py)_2$ and C about 15 for III·bipy and III·$(py)_2$. Inspection of molecular models of III and IV indicated that the interspin distance in an extended conformation of the molecule was about 9–10 Å for III and 10–12 Å for IV. (The results obtained in fluid solution suggest that the low-temperature form of the molecule is an extended form.) Even if the short ends of these ranges are used, substitution of the values of C and r into eq 3 indicates that the nickel relaxation time would have to be about 5×10^{-10} s, which seems unreasonably long for Ni(II). T_1 values of 10^{-11}–10^{-12} are commonly cited for Ni(II).[31,32] Thus both the inability to obtain good agreement between the calculated and observed line shapes and the need to invoke a surprisingly long metal T_1 indicate that the dipolar Leigh model does not adequately describe these spectra.

---

(30) Leigh, J. S., Jr. *J. Chem. Phys.* **1970**, *52*, 2608–2612.

(31) Friedman, H. L.; Holz, M.; Hertz, H. G. *J. Chem. Phys.* **1979**, *70*, 3369–3383.

(32) Swift, T. J. In "NMR of Paramagnetic Molecules"; LaMar, G. N.; Horrocks, W. deW, Holm, R. H., Eds.; Academic Press: New York, 1973; Chapter 2.

In light of the spectra discussed below for the shorter chain compounds it is likely that exchange interactions also play a significant role in the line broadening observed for the adducts of III and IV.

The spectra of the six-coordinate adducts of I and II bear no resemblance to normal frozen-solution nitroxyl EPR spectra. The nitroxyl lines are severely broadened and spread over several hundred Gauss. For I·bipy the low-field and high-field turning points are at 2600 and 3400 G, respectively (Figure 4A). The spectrum of I·$(py)_2$ is slightly more spread out (turning points at 2400 and 3600 G, respectively). Even for II (n = 1) the low-field and high-field turning points in the spectrum of II·$(py)_2$ are at 2900 and 3600 G, respectively. The spectra of the six-coordinate adducts of I and II do not saturate at the highest microwave powers available on our spectrometer. These observations indicate significant mixing of the nickel and nitroxyl wave functions.[33] CPK molecular models indicate that the interspin distances are about 7 and 8 Å respectively for the nitrogenous base adducts of I and II. The observed splittings in the spectra are too large to be explained by purely dipolar interaction at these distances. Thus it appears that a substantial exchange interaction must be invoked to explain the large shifts in the spectra.

The observation of large splittings in the frozen-solution spectra is noteworthy in another respect. We expect that when a nitroxyl interacts with a rapidly relaxing metal the appearance of the nitroxyl portion of the spin-coupled spectrum will be dependent on the rate of the metal relaxation compared with the splittings in the spectrum. When the metal relaxation rate is comparable to the splittings in the nitroxyl lines, a broadened spectrum is expected. When the metal relaxation rate is fast relative to the potential splittings of the nitroxyl lines, the splittings will be averaged out. In between these two limits, the widths of the nitroxyl lines should be a function of the metal relaxation rate and of the spin–spin interaction. These arguments are analogous to those used in the analysis of temperature-dependent EPR and NMR spectra of dynamic systems. Since information is not available concerning the nickel relaxation rates in these compounds and since the transitions have not been assigned, it is not possible to determine the extent to which the line shapes and line positions reflect the partial collapse of larger splitting due to a nickel relaxation rate which is not sufficiently rapid to completely average out the spin–spin interaction. Further studies are needed to estimate the metal relaxation times, zero field splittings, and exchange interactions in these molecules.

Conclusions

The nickel–nitroxyl interaction in nitrogenous base adducts of I–V decreases rapidly as n increases. However, even in V the spin–spin interaction is detectable. In fluid solution the flexible hydrocarbon chains in the compounds with n = 2, 4, or 6 permit intramolecular nickel–nitroxyl interactions which are strongly dependent on the solution viscosity. The large splittings in the frozen solution spectra of the six-coordinate adducts of I and II indicate that exchange makes a significant contribution to the spin–spin interaction.

Acknowledgment. This work was supported in part by NIH grant GM21156 and the donors of the Petroleum Research Foundation, administered by the American Chemical Society. We are grateful to Prof. Kosman (SUNY Buffalo) for providing us with unpublished details of the syntheses reported in ref 20 and to Prof. Hornback and Dr. More for helpful discussions concerning the syntheses.

Registry No. I, 85361-86-0; II, 85361-88-2; III, 88945-48-6; IV, 88945-49-7; V, 88945-50-0; VI, 88932-76-7; VII, 88932-77-8; VIII, 31146-15-3; IX, 88932-78-9; X, 88932-79-0; XI, 88932-80-3; XII, 88932-81-4; XIII, 88932-82-5; XIV, 88932-83-6; XV, 88932-84-7; XVI, 88932-85-8; XVII, 88932-86-9; XVIII, 88932-87-0; tempone, 2896-70-0; triethyl phosphonoacetate, 867-13-0; triethyl 4-phosphonocrotonate, 10236-14-3.

---

[33] Throughout the text the observed EPR lines are referred to as nitroxyl lines which is the assignment of the transitions in the limit as J approaches 0.

Redox Conduction in Single and Bilayer Films of Redox Polymer

P. G. Pickup,[‡] W. Kutner,[†] C. R. Leidner, and Royce W. Murray*

Contribution from Kenan Laboratories of Chemistry, University of North Carolina, Chapel Hill, North Carolina 27514. *Received August 8, 1983*

Abstract: Polymeric films made from Ru and Os polypyridine complexes and sandwiched between potential-controlled Pt and porous Au electrodes exhibit low resistance to current flow when the electrode potentials are such as to generate mixed-valent states in the polymers, and high resistances when the films are composed of only one oxidation state. The observed current–potential curves with their limiting currents can be understood in terms of a concentration gradient (not potential gradient) driven flow of electrons with effective mobility characterized by an electron diffusion coefficient D_{ct}. Sandwich-electrode measurements of D_{ct} for the M(III/II) mixed-valent state agree with those produced by other methods, and estimates from D_{ct} of effective electron self-exchange rates in the polymers come close to those known for homogeneous solution self-exchange rates between $[M(bpy)_3]^{n+}$ complexes. For poly$[Os(bpy)_2(vpy)_2]^{2+}$ films, the electron mobility varies in the proportion 1:3:25 for the three mixed-valent states Os(III/II), Os(II/I), and Os(I/0), respectively. The most highly conducting state can pass currents of 0.6 A/cm^2.

Our[1] and others'[2,3] interest in electron transport in thin films of electroactive polymers stems from fundamental questions about electron mobility in these materials and from its connection to potential applications of the films to electrocatalysis,[2i,4] photoelectrochemistry,[5] and chemical devices.[1h] When studied by transient methods,[1a,2b] the electron transport follows diffusion laws

Scheme I

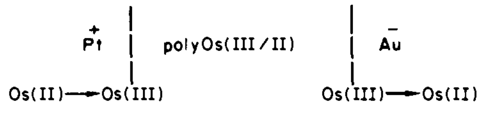

[†] Permanent address: Institute of Physical Chemistry, Polish Academy of Sciences, Kasprzaka 44,01-224 Warsaw, Poland.

[‡] Department of Chemistry, State University of New York at Buffalo.

0002-7863/84/1506-1991$01.50/0